Cholesterol Orientation and Tilt Modulus in DMPC Bilayers

George Khelashvili,*,† Georg Pabst,‡ and Daniel Harries*,§

Department of Physiology and Biophysics, Weill Medical College of Cornell University, New York, New York, Institute of Chemistry and the Fritz Haber Research Center, The Hebrew University of Jerusalem, Jerusalem, Israel, and Institute of Biophysics and Nanosystems Research, Austrian Academy of Sciences, A-8042 Graz, Austria

Received: March 2, 2010; Revised Manuscript Received: April 30, 2010

We performed molecular dynamics (MD) simulations of hydrated bilayers containing mixtures of dimyristoylphosphatidylcholine (DMPC) and cholesterol at various ratios, to study the effect of cholesterol concentration on its orientation, and to characterize the link between cholesterol tilt and overall phospholipid membrane organization. The simulations show a substantial probability for cholesterol molecules to transiently orient perpendicular to the bilayer normal, and suggest that cholesterol tilt may be an important factor for inducing membrane ordering. In particular, we find that as cholesterol concentration increases (1−40% cholesterol) the average cholesterol orientation changes in a manner strongly (anti)correlated with the variation in membrane thickness. Furthermore, cholesterol orientation is found to be determined by the aligning force exerted by other cholesterol molecules. To quantify this aligning field, we analyzed cholesterol orientation using, to our knowledge, the first estimates of the cholesterol tilt modulus χ from MD simulations. Our calculations suggest that the aligning field that determines χ is indeed strongly linked to sterol composition. This empirical parameter (χ) should therefore become a useful quantitative measure to describe cholesterol interaction with other lipids in bilayers, particularly in various coarse-grained force fields.

Introduction

An essential component of mammalian cell membranes, cholesterol is known to be critical for membrane organization, dynamics, and function.[1−5] The nonuniform distribution of cholesterol between cellular organelles,[3] lipid membrane compartments,[4,6−10] and even between leaflets of the same bilayer,[11] highlights cholesterol's role in influencing the biophysical properties of a fluid lipid matrix and in the stabilization and function of membrane proteins through specific interactions. The great variability found in the concentration of cholesterol among various cells and between the plasma membrane and the variety of membranes of other cellular organelles underscores the importance of tightly regulated cholesterol content for proper function at the subcellular level.[12,13] In fact, inborn errors of cholesterol synthesis lead to major developmental abnormalities, and conversely, an excess of cholesterol is widely acknowledged as detrimental.[14,15]

Experimentally, it has been shown that sterols have affinities for certain lipid types when introduced to lipid mixtures. A strong preferential interaction seems to exist for saturated phospholipids with phosphatidylcholine (PC) headgroups.[16] At least for moderate concentrations in PC membranes, cholesterol resides in the membrane such that the hydroxyl group is solvated in the lipid headgroup region, while the hydrophobic tail is buried deep in the hydrocarbon region of the lipids.[17,18] Theory and simulation show that cholesterol can be expected to be positioned in lipid membranes in a slightly tilted configuration,[19−25] with the hydroxyl group positioned in the lipid headgroup area.

However, this simple picture does not hold true, for example, when the membrane is composed of poly-unsaturated fatty acids (PUFAs). Recently, it was found that in the presence of lipids containing PUFAs, the cholesterol moiety, the sterol (aromatic) ring and its hydroxyl group, can situate deep inside the hydrocarbon region, lying either immersed in the membrane's hydrocarbon core or possibly in a flipped orientation.[16] It is possible that the restrictive nature of the cholesterol molecule prohibits the approach of disordered PUFA chains: the entropic penalty created by the steric interactions with the planar rigid cholesterol molecules oriented along the membrane normal becomes too large. Moreover, a recent combined X-ray scattering and molecular dynamics study of cholesterol at 0.4 mole fraction in thin, short-chain monounsaturated diC14:1PC lipid bilayers[26] showed multiple instances when cholesterol molecules transiently orient perpendicular to the bilayer normal, with the hydroxyl group submerged in the center of the bilayer. However, this study showed that "lying down" of cholesterol was absent in mixtures containing the longer-chained diC22:1PC lipid. This evidence clearly underscores the interplay between the forces that act on the cholesterol molecule and the forces with which it acts on its lipid environment.

Here we focus on mixtures of cholesterol (Chol) in dimyristoylphosphatidylcholine (DMPC) lipids, a 14-carbon disaturated lipid that possesses a neutral (zwitterionic) PC headgroup (see Figure 1). To further explore cholesterol's tilt degree of freedom and its effect on membrane structural properties, we have produced and analyzed trajectories from molecular dynamics (MD) simulations of DMPC−Chol mixed bilayers at different sterol concentration. We find that Chol molecules in DMPC membranes frequently transiently orient perpendicular to the bilayer normal, similar to their

* To whom correspondence should be addressed. Phone: 212-746-6539 (G.K.); Phone: 972-2-6585484 (D.H.). Fax: 212-746-6226 (G.K.); Fax: 972-2-6513742 (D.H.). E-mail: gek2009@med.cornell.edu (G.K.); E-mail: daniel@huji.ac.il (D.H.).
† Weill Medical College of Cornell University.
‡ Austrian Academy of Sciences.
§ The Hebrew University of Jerusalem.

10.1021/jp101889k © 2010 American Chemical Society
Published on Web 05/19/2010

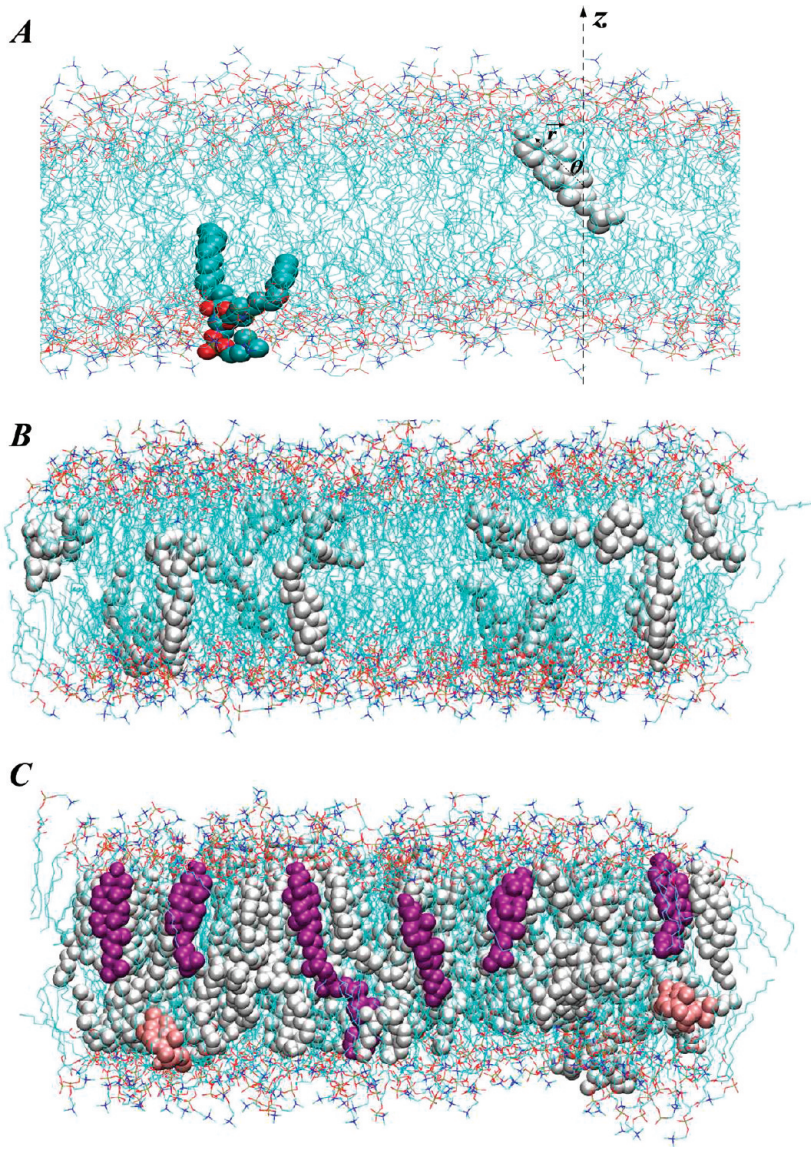

Figure 1. (*A*) Fragment of simulated DMPC−cholesterol bilayer at 10% Chol concentration showing the definition of cholesterol tilt angle. For clarity, only one cholesterol molecule is shown (in white), and water molecules are removed. For illustration purposes, one DMPC lipid molecule is also highlighted in space-fill. The tilt angle θ of cholesterol is defined as the angle between the cholesterol ring plane vector $\vec{r}$ (connecting Chol C3 and C17 atoms) and z axis of the simulation box. Panels (*B*) and (*C*) depict snapshots of DMPC−cholesterol bilayers at 5 and 30% Chol contents, respectively, and illustrate the different level of cholesterol organization in high and low Chol content membranes. On both panels, DMPC lipids are shown as lines, and cholesterols are depicted in space-fill. Chols in purple in panel (*C*) highlight increased long-range orientational order of cholesterols in the 30% mixture compared to that in 5%. However, note that some instances still can be found, even at 30% Chol, when cholesterol molecules transiently orient perpendicular to the bilayer normal (pink colored space-fill in panel *C*).

behavior in diC14:1PC bilayers[26] (lipids differing only by a single double bond in each hydrocarbon chain), suggesting that, at least at high sterol content, cholesterol orientation in DMPC and diC14:1PC may be similar.

Our study further suggests that cholesterol tilt may be an important factor capable of inducing membrane ordering. In particular, we find that, as Chol concentration increases, the change in average cholesterol orientation is strongly (anti)correlated with the concomitant increase in membrane thickness and that this correlation persists for the wide cholesterol content range studied (1−40% Chol). Notably, over this range of concentrations and for temperatures above the main fluid-to-gel phase transition temperature of pure DMPC lipid (∼297 K[27]), DMPC−Chol mixtures are known to transition through different levels of organization as a function of cholesterol concentration.[27] Specifically, for sterol compositions lower than ∼10%, DMPC−Chol mixtures exhibit fluid-like properties; at moderate Chol densities (between ∼10 and ∼30% Chol), the temperature−composition diagram[27] predicts coexistence of fluid and Chol-rich liquid-ordered states; and last, at the high Chol concentration regime (above ∼30% Chol), DMPC−cholesterol mixtures are expected to be in the one-phase liquid-ordered state. We have been able to relate cholesterol's preferred orientation to these fluidity states, thereby establishing a link between cholesterol orientation and the well-known lipid condensing effect.[28,29]

We also find that cholesterol orientation is strongly determined by the aligning force induced by other cholesterol molecules, somewhat similar to the density-induced "lying down" to "standing up" transitions that are observed in Langmuir monolayers.[30,31] This aligning field is discussed in terms of a cholesterol tilt modulus calculated here for the first time from MD simulations.

TABLE 1: Duration of Equilibration and Production Phases for All Simulated Mixtures

system	equilibration (ns)	production (ns)
0% Chol	10	15
1% Chol	10	35
3% Chol	10	30
5% Chol	10	30
10% Chol	25	20
20% Chol	25	20
30% Chol	20	20
40% Chol	15	17

Computational Methods and Procedures

Model Systems and Simulation Details. MD simulations were performed on hydrated (14:0) DMPC−cholesterol mixtures at 0, 1, 3, 5, 10, 20, 30, and 40% Chol concentrations. Our choice of lipid is dictated by several factors: DMPC is a widely studied phospholipid and forms a good basis for comparing our computational results with experiments[29,32−34] and also with previous model calculations;[20,23,24] the system is particularly amenable to physicochemical studies because of its relatively low gel-to-fluid transition temperature;[27] and last, DMPC is generally considered a "good" solvent for cholesterol, so that studies of these mixtures should provide a setting for discussing the effects of cholesterol on lipids that generally do not segregate away from it in multicomponent membranes.

The bilayers were constructed from previously equilibrated pure DMPC membranes containing 100 lipids at a temperature $T = 303$ K.[35] To build the model systems, the DMPC bilayer was first depleted from all solvent molecules and replicated four times in the membrane plane. Appropriate cholesterol fractions were then created by randomly substituting phospholipids with Chol molecules oriented along the bilayer normal. After hydration, the final mixtures all contained 200 molecules per monolayer leaflet and were solvated by ∼32 SPCE water molecules per lipid headgroup.

All simulations were performed using the GROMACS simulation suite.[36,37] The LINCS algorithm was used to constrain all bond lengths[38] allowing for 2 fs time steps. Periodic boundary conditions were applied in all three dimensions, and long-range electrostatics were calculated using the Particle-Mesh-Ewald algorithm.[39] A cutoff of 18 Å was employed for van der Waals interactions. The systems were simulated in an NPT ensemble. A constant pressure of 1 atm was maintained using the Parrinello−Rahman semi-isotropic pressure coupling scheme.[40,41] The simulations were performed at $T = 308$ K (corresponding to a reduced temperature $(T - T_0)/T_0$ of 0.039, T_0 being the DMPC fluid-to-gel phase transition temperature) using the Noose−Hoover temperature coupling method.[42] By simulating DMPC/Chol bilayers at 308 K and for various sterol concentration we expect to explore different regimes of fluidity in these mixtures, according to the previously proposed temperature−composition diagram for DMPC/cholesterol membranes[27] (see Results and Discussion).

For each model system, an equilibration phase was performed at $T = 308$ K and with velocity reset frequency of 100 ps, followed by a continuous production run. The lengths of the equilibration and production phases for different membrane mixtures are summarized in Table 1. The recently improved united atom GROMOS96 43A1 force-field was utilized throughout. This parameter set, described in detail in ref 35, has been successfully tested for various lipid membrane systems[35,43] and is publicly available from http://www.nanoconductor.org.

Evaluating Cholesterol Tilt Angle Probability Distributions Plots. The orientation of cholesterol molecules in the membrane is described here using the unit vector $\hat{\mathbf{n}}$ of the vector joining C3−C17 groups on Chol ring, commonly used to describe cholesterol tilt, and the bilayer normal (see Figure 1*A*). This vector is described in the lab (simulation box) reference frame in polar coordinates by the angle θ, defined as the angle between $\hat{\mathbf{n}}$ and the bilayer normal z axis. As usual for polar coordinates, θ is defined in the range [0°; 180°]. In this definition $\theta = 0°$ represents a cholesterol orientation where the ring plane is parallel to the bilayer normal z axis. An additional polar angle ϕ, describing the angle that the projection of $\hat{\mathbf{n}}$ on the xy plane makes with the x axis of the simulation box, varries within [0°; 360°]. Note that any angle θ can have multiple values for ϕ. The number of available states grows with θ in the [0°; 90°] range, because the vector $\hat{\mathbf{n}}$ can circumscribe larger circles for larger θ.

To investigate cholesterol orientation in different compositional mixtures, we examined cholesterol tilt angle distributions (see Results and Discussion). To this end we constructed normalized probability densities $P(\theta)$ (summed for each θ over all ϕ angles) of cholesterol tilt angle in DMPC/Chol membranes of various sterol content (Figure 5*A*). To obtain probability densities, the [0°; 180°] angular interval for θ was divided into 180 bins with size $\delta\theta = 1°$, and a cholesterol orientational angle histogram was collected for each system. The histograms were then normalized by the total number of entries to obtain the $P(\theta)$ distributions. By construction, $P(\theta)$ is symmetrical around $\theta = 90°$.

We note that distribution plots like the ones shown in Figure 5*A* are generally strongly dependent on the extent of sampling during the simulation. To ensure adequate sampling in mixtures containing a small number of Chol molecules, these systems were allowed to propagate in the production phase for longer periods compared to bilayers containing high concentrations of cholesterol (see Table 1). To judge the sampling quality, we monitored for all simulated systems the number of times a cholesterol molecule visits a certain $[\theta, \theta + \delta\theta]$ angular bin. For instance, we found that in the 1% Chol mixture, each cholesterol molecule visits any $[\theta, \theta + \delta\theta]$ bin for $\theta \in [10°, 60°]$ more than 200 times for the duration of the production run. Overall, in all mixtures on average cholesterol molecules sampled each $[\theta, \theta + \delta\theta]$ bin for $\theta \in [8°, 60°]$ at least 90 times. Therefore, we safely assume that all $P(\theta)$ distributions are well-converged, at least for $\theta \in [8°, 60°]$.

Results and Discussion

Structural Properties of Model DMPC/Cholesterol Bilayers Validated by Experiments. Figure 1*B* and *C* illustrate final snapshots of simulated 5 and 30% Chol mixtures and highlight the different levels of cholesterol organization in low and high Chol-containing membranes. In particular, with increasing concentration, cholesterol molecules appear to exhibit long-range orienational order around the bilayer normal. At the same time, the membrane overall appears to become more condensed lateraly and concomitantly becomes thicker. To quantitatively characterize and validate our simulations, we computed several key structural properties of the model bilayers including X-ray form factors, electron densities, NMR order parameters, as well as molecular areas and volumes.

Figure 2 compares form factors $F(q)$ derived from our MD simulations to those from small-angle X-ray scattering (SAXS) experiments of DMPC at a temperature of $T = 308$ K and in the presence of various cholesterol concentrations (as previously

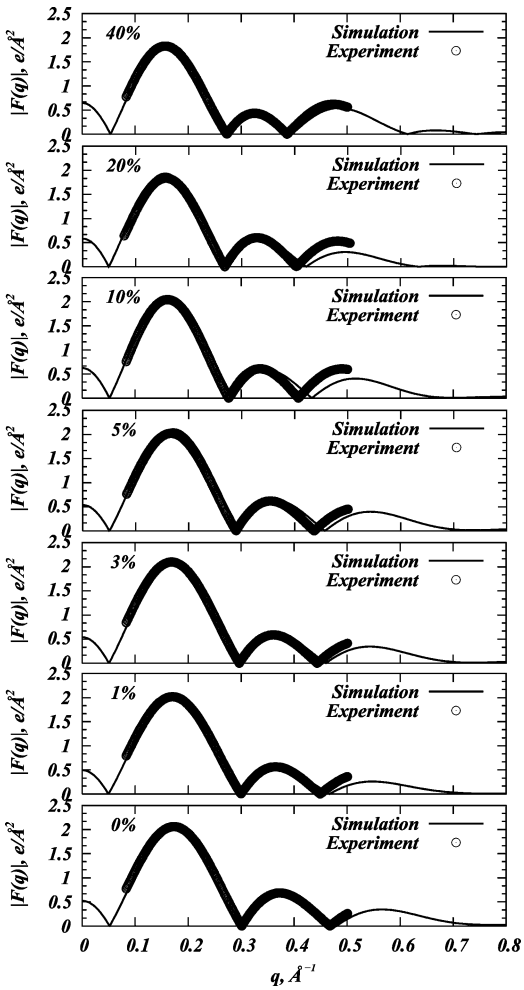

Figure 2. Comparison of experimental and simulation form factors $F(q)$ for DMPC−cholesterol mixtures in the presence of 0, 1, 3, 5, 10, 20, and 40% Chol. $F(q)$s computed in small-angle X-ray scattering (SAXS) experiments were obtained from ref 32 and are shown as symbols. MD form factors are depicted as solid lines.

described in ref 32). For the SAXS experiments, form factors were calculated from X-ray scattering intensities.[32,44−47] To obtain $F(q)$ from simulations, the electron density profile for each model membrane was first constructed by dividing the simulation cell into slabs in the z direction, and the number of electrons corresponding to the atoms in each slab was counted. The corresponding form factors were then evaluated using the following expression:

$$F(q) = \int_{-D/2}^{D/2} (\rho_e(z) - \rho_e^{bulk}) \cos(qz) dz \qquad (1)$$

where D is the average length of the simulation cell in the z direction, $\rho_e(z)$ is the symmetric electron density of the system, and ρ_e^{bulk} is the electron density of bulk water.

Figure 2 illustrates the remarkable agreement between SAXS and simulation data for all DMPC/Chol mixtures, at least for the first two lobes of the form factor. (Note that no SAXS data were available for 30% DMPC/Chol.) Furthermore, these plots reveal that upon increasing cholesterol concentration, the maxima of the form factors shift toward lower q values, giving rise to additional peaks in the high q-range. These features are usually indicative of bilayer thickening and suggest increased ordering within the membrane.

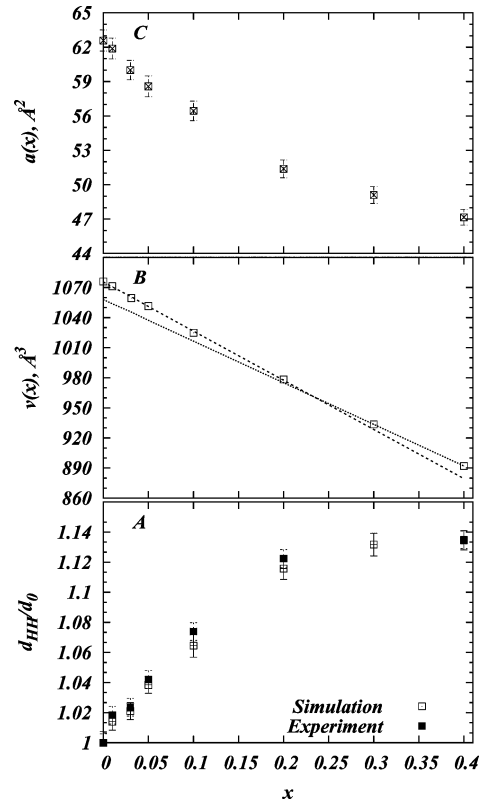

Figure 3. (*A*) Comparison of experimental[32] and simulation peak-to-peak distances (d_{HH}) from the electron density profiles for different DMPC/cholesterol mixtures. The panel shows d_{HH} normalized by the thickness of the pure DMPC bilayer d_0 in experiment and simulations. (*B*) Volume per molecule $v(x)$ as a function of cholesterol concentration (symbols). Two lines represent linear fits to the data in two cholesterol concentration regimes: $x \leq 0.2$ and $x > 0.2$, respectively. (*C*) Change in area per molecule $a(x)$ with cholesterol fraction.

The trend is even more apparent in the electron density and lipid tail NMR order parameter profiles. Specifically, a peak-to-peak (or head−head[33]) distance in the electron density can be assigned to an average separation between phosphate atoms on lipids from opposite leaflets and, thus, provides a measure of bilayer thickness. In Figure 3*A*, we present head−head distances derived from the model electron density profiles (normalized by the thickness of the pure DMPC bilayer derived from simulation) versus cholesterol content in different DMPC/Chol mixtures. For comparison, the panel also shows the same measure, as calculated from the SAXS experiments[32] (normalized by the thickness of the pure DMPC bilayer derived from the experiment). Figure 3*A* illustrates near perfect agreement between MD simulations and the SAXS data and confirms the well-established observation for fluid bilayers, whereby upon Chol addition, the membrane thickness increases with composition in a nonlinear fashion.[29,33,48−51] Furthermore, Figure 3*A* reveals that the bilayer thickness starts saturating at around 20% Chol. Similar progression has been observed in recent X-ray diffraction studies on DMPC/cholesterol mixtures at $T = 303$ K and at different hydration levels.[29,33] Overall, in our simulations 40% cholesterol thickens DMPC bilayers by ∼5.3 Å, a value close to that previously reported.[29,32−34]

Bilayer thickening upon cholesterol addition is due to ordering of the lipid hydrocarbon chains, as illustrated in the simulated deuterium order parameter: S_{CD} plots in Figure 4. The order parameters for (saturated) carbons on the hydrocarbon tails of DMPC lipid in simulations that use the united atom force field is determined by[52]

$$-S_{CD} = \frac{2}{3}S_{xx} + \frac{1}{3}S_{yy} \quad (2)$$

where S_{xx} and S_{yy} are the components of the order parameter tensor

$$S_{ij} = \frac{1}{2}\langle 3 \cos \alpha_i \cos \alpha_j - \delta_{ij}\rangle \quad ij = x, y, z \quad (3)$$

α_i being the angle made by the ith molecular axis with the bilayer normal and δ_{ij} representing the Kronecker delta function.

Consistent with our electron density profiles and in line with experimental[18,33,53−57] and theoretical[20,21,23,24,58,59] data on DMPC/Chol mixtures, Figure 4 reveals that the ordering of hydrocarbon chains of DMPC lipid increases with cholesterol content and saturates at ≈20% cholesterol.

Another key structural property of mixed membranes is the partial molecular volumes of individual bilayer components, that is, the partial volumes of DMPC, V_{DMPC}, and cholesterol, V_{Chol}. In the spirit of the derivation presented by Greenwood et al,[28] we evaluate the partial molecular volumes by first expressing the total volume of the simulation box as

$$V_{BOX} = N_W V_W + ((1 - x)V_{DMPC} + xV_{Chol})(N_{DMPC} + N_{Chol}) \quad (4)$$

where N_W and $V_W = 30.5$ Å^2 are the number of waters and volume of a single water molecule, respectively,[35] and $x = N_{Chol}/(N_{DMPC} + N_{Chol})$ is the number fraction of cholesterol in the mixture. We then calculate the volume per lipid in the bilayer at each Chol concentration using[28,43]

$$v(x) = \frac{V_{BOX} - N_W V_W}{N_{DMPC} + N_{Chol}} = V_{DMPC} + x(V_{Chol} - V_{DMPC}) \quad (5)$$

Figure 3*B* shows the volumes $v(x)$ versus cholesterol fraction x. The plot reveals a near linear decrease in $v(x)$ with Chol content, indicating a "condensing" effect of cholesterol, as described in ref 28. Furthermore, similar to the experimental measurements by Greenwood et al. on DMPC/Chol mixtures at $T = 303$ K, we find that our data can be well represented by a double linear fit to the volumetric data that corresponds to $x \leq 0.2$ and $x > 0.2$ concentration ranges (Figure 3*B*). Using eq 5, the values of the slope and intercept of each fitted line can be used to obtain two sets of values for V_{DMPC} and V_{Chol}, corresponding to the partial molecular volumes of DMPC and Chol in the two concentration regimes.[28,43] Table 2 compares V_{DMPC} and V_{Chol} derived from the linear fits to the data in Figure 3*B* with those obtained in ref 28. Overall, we find good agreement between partial molecular volumes from MD and experimental data.

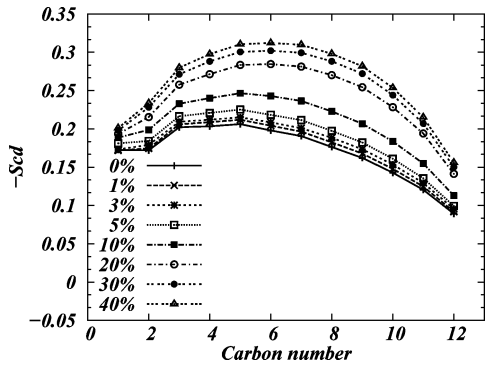

Figure 4. Deuterium order parameter profiles derived from simulations, averaged over two hydrocarbon chains of DMPC lipid at different cholesterol concentrations.

TABLE 2: Partial Molecular Volumes (in Å^3)[a]

	MD	expt[28]
temperature	308 K	303 K
V_{DMPC}	1075.50 ($x \leq 0.2$)	1099.6 ($x < 0.25$)
V_{Chol}	585.25 ($x \leq 0.2$)	565.1 ($x < 0.25$)
V_{DMPC}	1057.97 ($x > 0.2$)	1076.8 ($x \geq 0.25$)
V_{Chol}	643.15 ($x > 0.2$)	637.5 ($x \geq 0.25$)

[a] Calculated from Figure 3*B*.

To further explore the condensing effect of cholesterol on DMPC membranes, we evaluated the area per molecule $a(x)$, defined as

$$a(x) = \frac{A_{BOX}}{N_{DMPC} + N_{Chol}} \quad (6)$$

where A_{BOX} is the total area of the membrane.

Figure 3*C* shows $a(x)$ as a function of cholesterol concentration. In agreement with experiments[29] and modeling studies[51] of DMPC−cholesterol mixtures, we find a strong nonlinear decrease in molecular area with increasing cholesterol content, indicative of the previously described cholesterol condensation on DMPC lipids.[29] Taken together, the structural data presented in Figures 2−4 provide a strong basis to conclude that all simulated bilayer mixtures are good models for further investigation of molecular properties. With that, we now proceed to the principal findings from our work.

Cholesterol Orientation in DMPC Bilayers. ***Average Cholesterol Tilt Angle.*** Figure 5*A* shows normalized probability densities $P(\theta)$ (see Computational Methods and Procedures) of cholesterol tilt angle in DMPC/Chol membranes for various sterol concentrations. For comparison, Figure 5*A* also includes the expected probability density distribution of tilt angles in a hypothetical "ideal gas" of cholesterols, where noninteracting Chol molecules are oriented randomly, so as to maximize number of states accessible to them. Obviously, this random distribution is given by $P_0(\theta) = \sin \theta$, since the number of possible orientations that any vector making an angle θ with the z axis can assume is degenerate by a factor $\sin \theta/2$, and the range of tilt angles in Figure 5*A* is [0; 90°] (see below for more details). For each sterol composition, we also calculated the average cholesterol tilt angle, defined as

$$\langle\theta\rangle = \int_0^{90^\circ} \theta P(\theta) d\theta \quad (7)$$

Note that, in principle, the average cholesterol tilt angle can be defined in several ways, and the definition employed here may differ from the ones used in other MD studies[20,22−26,60]

We first discuss the values of $\langle\theta\rangle$, as presented in Table 3, before examining the distribution plots themselves in more detail. The progression of $\langle\theta\rangle$ indicates that the average cholesterol tilt decreases with increasing cholesterol content. This is in line with the results from electron spin resonance (ESR) experiments,[61] and NMR[62] studies of different

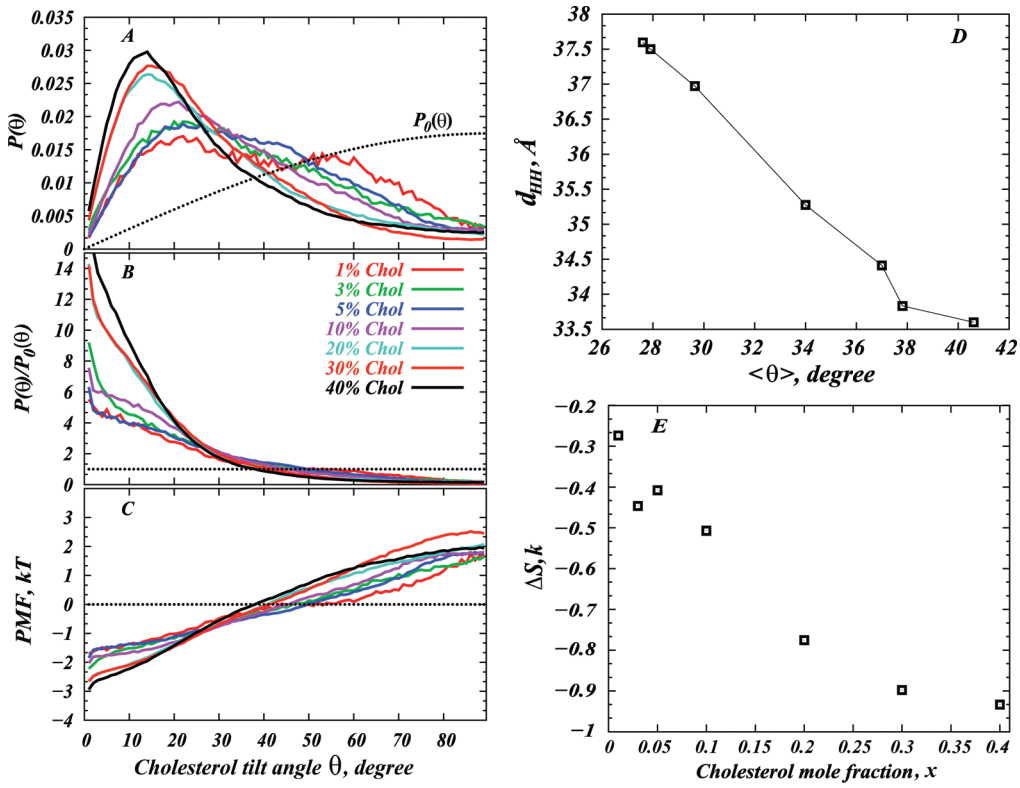

Figure 5. (*A*) Normalized probability distributions $P(\theta)$ of cholesterol tilt angle in DMPC/Chol membranes of various sterol concentrations. The tilt angle is defined as the angle between the vector describing cholesterol ring plane orientation and the bilayer normal (see Computational Methods and Procedures). For comparison, we also plot the expected distribution of tilt angles in a noninteracting system of Chol molecules where cholesterols are oriented randomly. This random distribution is given by $P_0(\theta) = \sin\theta$. (*B*) Plots of $P(\theta)/P_0(\theta)$ for different DMPC/cholesterol mixtures derived from panel *A*. (*C*) Potential of mean force (PMF) plots from the distributions in panel *B* (see text for details). (*D*) Correlation between average cholesterol tilt $\langle\theta\rangle$ and bilayer thickness d_{HH} in simulated systems (lines are guides to the eye). (*E*) Loss in cholesterol orientational entropy with increasing cholesterol concentration.

TABLE 3: Average Tilt Angles, $\langle\theta\rangle$[a]

cholesterol fraction	avg tilt angle (°)
0.01	40.6
0.03	37.8
0.05	37.5
0.1	30.4
0.2	29.6
0.3	27.9
0.4	27.6

[a] Calculated from eq 7 and $P(\theta)$ distributions in Figure 5*A*.

phospholipid(PC)−Chol systems. These studies suggest that the orientational ordering of cholesterol in PC−Chol mixtures indeed increases with sterol concentration. In fact, according to ref 61, this trend is most prominent for DMPC membranes among saturated PCs of different hydrocarbon tail length.

Cholesterol Tilt Correlates with Bilayer Thickness. To examine how changes in average cholesterol orientation upon increasing Chol concentration relate to the concomitant variation in membrane thickness, Figure 5*D* shows the head−head distance d_{HH} (as presented in Figure 3) versus $\langle\theta\rangle$. Remarkably, the plot reveals that sterol tilt and membrane thickness are strongly anticorrelated. Because bilayer thickness is directly related to ordering of lipid tails, these results suggest that sterol tilt is an important indicator of the order that cholesterol can induce in the membrane (see below for further discussion). The correlation between cholesterol tilt and membrane ordering persisted over the entire 1−40% cholesterol concentration range that we have simulated. These results are in general agreement with MD studies by Aittoniemi et al.[22] that examined instantaneous tilt angle of a sterol as a function of the corresponding average molecular order parameter of neighboring lipid chains in 20% DPPC−Chol and DOPC−Chol mixtures. These authors found a similar correlation between the two properties.

Interestingly, over the 1−40% range of cholesterol concentrations and at $T = 308$ K, DMPC−cholesterol bilayers are known to undergo different levels of organization with changes in cholesterol content.[27] Namely, for sterol concentrations lower than ∼10%, DMPC−cholesterol mixtures exhibit fluid-like properties; at moderate Chol densities (between ∼10 and ∼30% Chol), the temperature−composition diagram[27] predicts coexistence of fluid and Chol-rich liquid-ordered states, and last, at high Chol concentration regime (above ∼30% Chol), DMPC−cholesterol mixtures are expected to be in the one-phase liquid-ordered state. Figure 5*D* indicates that cholesterol's ability to affect membrane ordering in various fluidity states is strongly correlated with cholesterol's preferred orientation.

Cholesterol Alignment with Increasing Concentration as a Possible Mechanism for Membrane Ordering. To learn how sterol orientation may contribute to lipid tail ordering, we now examine in more detail the $P(\theta)$ functions, as plotted in Figure 5*A*, for various DMPC/Chol mixtures. In the limit of low Chol concentration (1−5% Chol), the tilt angle distributions are broad. As sterol content increases, $P(\theta)$ appears to develop a well-defined maximum at lower tilt angles, and the distributions become narrower, indicating stronger alignment of cholesterol molecules along the bilayer normal. This behavior appears to be analogous to the well-known isotropic−nematic (I−N) transition in liquid crystals,[30] where hard-rod molecules assume

preferred orientation upon increased concentration (compare Figure 1*B* and *C*).

To understand the mechanism of cholesterol alignment, it is essential to consider several major factors that can contribute to the overall orientation of cholesterol molecules in the membrane. Pairwise interactions between sterol molecules and between Chol and PC tend to separate cholesterol molecules from each other, because Chol−Chol pair interactions are in general less favorable energetically compared to Chol-PC interactions (see, for instance, ref 63). In fact, this circumstance gave rise to the idea of cholesterol forming complexes with phospholipids.[64,65] In addition to this energetic factor, and similar to simple hard-rod molecules, each cholesterol also possesses degrees of freedom associated with orientational and translational entropy of the molecule inside the membrane. As cholesterol tilts at an angle θ from the bilayer normal, it can span more configurations compared to the position where it is upright. This degeneracy, which is proportional to $\sin\theta$, would in principle cause an isotropically oriented cholesterol molecule to preferably assume orientations that are perpendicular to the bilayer normal. Obviously, this ideal behavior, governed purely by entropic tendencies, will occur only in a hypothetical system of noninteracting Chol molecules, where all cholesterols would eventually orient themselves randomly, resulting in the $P_0(\theta)$ distribution shown in Figure 5*A* (dotted line). Indeed, the $P(\theta)$ plots in Figure 5*A* indicate that at low sterol compositions, where the Chol−Chol interaction effects are small, cholesterol is tilted, probably due mainly to the orientational entropy contribution that largely determines the maximum number of (tilted) states. This point can be clearly observed by comparing $P(\theta)$ for 1% Chol with the random distribution $P_0(\theta)$. Remarkably, these two distributions nearly coincide for the $\theta \in [45°, 60°]$ interval, indicating that for 1% Chol the probability of finding cholesterol molecules tilted with respect to the vertical at any angle within this angular range is the same as for randomly oriented noninteracting molecules.

In the membrane environment, however, the preferred cholesterol configuration is dictated by an interplay between all the energetic and entropic contributions described above. As cholesterol concentration increases, these molecules can be expected to preferentially "stand up" in the membrane. This tendency is first due to the sterol's attempt to gain "free volume" and hence translational entropy at the expense of orientational entropy. It can also result from lipid-mediated unfavorable chol−chol interactions that can be enthalpic in nature.

In an effort to avoid each other, sterols can align along the bilayer normal (see below). Thus, a nematic-like ordering of Chol molecules is established, where cholesterols do not directly interact with each other but instead become engaged in interactions with neighboring lipids. As a consequence, with increasing Chol concentration, condensation of cholesterols on DMPC lipids occurs[28,29] and lipid hydrocarbon chains concomitantly become more ordered (Figure 4), while the bilayer thickens (Figures 3 and 5*D*).

To quantify losses in cholesterol orientational entropy upon increasing Chol concentration, we defined the orientational entropy $\Delta S = \Delta S(x)$[66,67]

$$\Delta S = -k_B \int_0^{90°} P(\theta) \ln\frac{P(\theta)}{\sin\theta} d\theta \qquad (8)$$

and in Figure 5*E* we show ΔS as a function of cholesterol concentration. Note that this orientational entropy loss, as defined in eq 8, vanishes if Chol molecules are randomly oriented.[66,67] However, in DMPC/cholesterol membranes, ΔS is expected to deviate from zero due to the anisotropic orientation of cholesterols that reflect losses in orientational entropy. Indeed, Figure 5*E* reveals that for all mixtures ΔS is negative, and the orientational entropy decreases with increasing Chol concentrations. Furthermore, the change in ΔS is nonlinear and appears to be closely related to the change in membrane thickness (Figures 3*A* and 5*D*).

The observed loss in cholesterol orientational entropy upon change in concentration is consistent with theoretical predictions on energetics of single cholesterol transfer *between* bilayers containing different lipids[68] as well as on free energies of single cholesterol *desorption* from membranes consisting of different lipids.[69] In particular, using MD simulations, Zhang et al.[68] carried out free energy calculations of cholesterol transfer from a bilayer containing unsaturated palmitoyl-oleoyl-phosphatidylcholine (POPC) lipids to a bilayer consisting of ordered sphingomyelin (SM) lipid molecules. The process of transfer was found to be exothermic, suggesting that Chol transfer from POPC to SM was favorable energetically but prohibitive entropically. Furthermore, the authors predicted a broader distribution of cholesterol tilt in the POPC bilayer compared to that in the SM membrane, indicative of loss of rotational entropy upon Chol transfer from POPC to SM. Notably, the POPC/Chol and SM/Chol membranes discussed in ref 68 exist in different fluidity states so that the process of cholesterol exchange between these membranes can be deemed similar to Chol transfer from our low concentration DMPC/Chol mixtures to high Chol content DMPC/Chol membranes. Thus, in both types of mixtures, preferential cholesterol alignment in the high concentration regime (ordered state) is driven by sacrificing sterol's orientational freedom in favor of other free energy gains.

Bennett et al.[69] utilized atomistic as well as coarse-grained MD simulations to calculate free energies of cholesterol desorption from various PC membranes, as well as sterol flip-flop rates. These authors found that the free energy of cholesterol desorption from saturated lipid bilayers was higher than that from membranes containing polyunsaturated lipids. At the same time, the rate of cholesterol flip-flop was reduced with increasing lipid tail order. Consistent with our results for low-Chol mixtures, and as noted in ref 69, the trends observed by Bennett et al. are directly related to the fact that cholesterol in disordered environments, as found near polyunsaturated lipids, can orient itself perpendicular to the bilayer normal and reside close to the membrane center, where it has greater orientational freedom compared to the low orientational entropy "standing up" configuration.[70]

To better quantify cholesterol alignment in DMPC membranes, we defined the cholesterol orientational order parameter σ[31] as

$$\sigma = (1/2)(3\cos^2\beta - 1) \qquad (9)$$

Here β denotes the angle between the vectors defining the ring planes of two cholesterols (see Computational Methods and Procedures). Thus, $\sigma = 1$ if Chol molecules are perfectly aligned and $\sigma = 0$ for the orientationally isotropic mixture.[31] In Figure 6, we show σ as a function of the distance between cholesterol pairs for different mixtures. The plot clearly illustrates that for high concentrations (30%) orientational ordering of Chol molecules persists over large distances (see also Figure 1*C*). However, as Chol concentration decreases, orientational order weakens, and for small Chol fractions (3%) σ fluctuates strongly

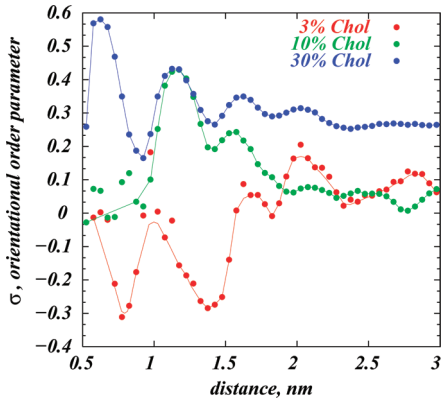

Figure 6. Cholesterol orientational order parameter σ (see text) as a function of distance between cholesterols. Results for 3, 10, and 30% systems are shown as circles, and the lines represent guides to the eye.

between low and negative values (Figure 1*B*) that correspond to a "lying down" configuration. Thus, cholesterol's behavior in the membrane is somewhat reminiscent of the orientational transformations of so-called Langmuir monolayers of amphiphilic molecules at the air−water interface (see ref 31 and references therein).

Cholesterol can "Lie Down" in DMPC Membranes. Remarkably, $P(\theta)$ plots reveal a nonzero probability for finding cholesterol molecules at very large tilt angles (Figure 5*A*), even for the highest sterol concentrations that we have simulated. We find many instances where cholesterol molecules in DMPC membranes transiently orient perpendicular to the bilayer normal (see Figure 1*B*,*C*). This result is interesting in light of recent experimental and simulation data on membranes containing polyunsaturated fatty acids (PUFA)[16] and diC14:1PC lipids.[26] These studies show that, in the presence of PUFAs or short-tail diC14:1PC lipids, the cholesterol with its aromatic ring and the hydroxyl group can reside deep inside the hydrocarbon region, lying either immersed in the membrane's hydrocarbon core or possibly in a flipped orientation.[16] Further, comparing diC14:1PC lipid-containing membranes to longer-tail diC22:1PC bilayers, both at 40 mol % Chol, Kučerka et al.[26] suggested that such cholesterol reorientations are mainly characteristic of thin membranes. Our data agree well with the findings in that study and suggest that cholesterol orientation in DMPC and diC14:1PC (these lipids differing only by a single double bond in each hydrocarbon chain) may be similar, at least at high sterol content.

Cholesterol Orientation is Related to Sterol Depth in the Membrane. Analyzing the positioning of cholesterols in different mixtures, we found that the change in cholesterol tilt upon increasing sterol concentration is linked to the vertical location (depth) of the cholesterol in the membrane, as detailed in Figure 7. For five DMPC/Chol mixtures, we show the normalized 2D probability densities (*color shades*) of finding cholesterol molecules with a tilt angle of θ (*vertical axis*) and with its hydroxyl (OH) group at a vertical distance h from the bilayer midplane (*horizontal axis*).[71] Thus, $\theta = 0$ describes cholesterol with its ring plane parallel to the bilayer normal, and $h = 0$ corresponds to the cholesterol OH group at the membrane midplane. Figure 7 shows a broad distribution in both tilt angle and OH group location for the low 3% Chol mixture, with an absence of a clear preferred orientation and most probable OH depth. But as cholesterol concentration increases, a most probable location of the hydroxyl group emerges. This maximum shifts toward the lipid headgroup region as Chol concentration

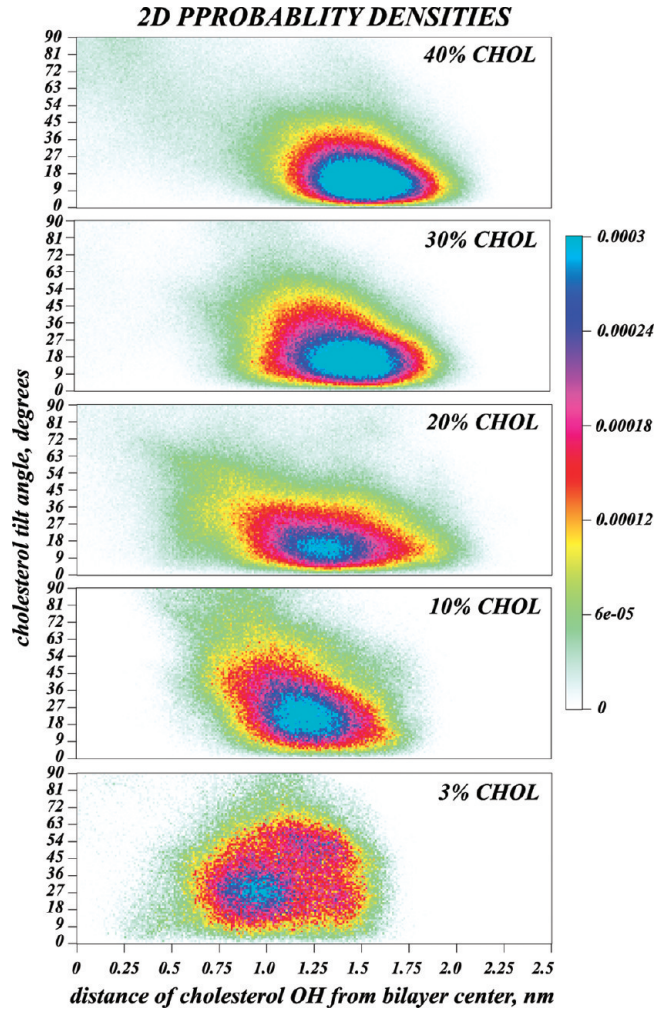

Figure 7. Normalized 2D probability densities (*color shades*), for selected systems, of finding a cholesterol molecule in a configuration with a tilt angle of θ (*vertical axis*) and with its hydroxyl (OH) group at a vertical distance h from the bilayer midplane (*horizontal axis*). $\theta = 0$ describes cholesterol with its ring plane parallel to the bilayer normal, and $h = 0$ corresponds to the cholesterol OH group at the membrane center.

rises further and eventually centers around $h \sim 1.25$ nm from the bilayer midplane for 40% Chol, in complete agreement with recently published results based on X-ray studies of PC/Chol monolayers.[72] At the same time, the broad angular distribution observed at 3% Chol also appears to merge into a single, narrower distribution of most probable angles.

Potential of Mean Force and Cholesterol Tilt Modulus in DMPC Bilayers. Our inferences so far highlight the competition between the entropic factors that tend to maximize the number of accessible states by orienting cholesterol molecules randomly at low cholesterol concentrations and aligning them at higher concentrations and the energetic forces that are dominated by unfavorable Chol−Chol interactions. At low Chol densities, both translational and rotational entropic contributions dominate. But as sterol concentration rises, the energetic factor, together with the translational entropy factors become more prominent, and the $P(\theta)$ distributions gradually diverge from the random distribution (Figure 5*A*). This trend is more apparent from Figure 5*B*, where we show the ratio of $P(\theta)$ from Figure 5*A* to the $P_0(\theta) = \sin\theta$ factor. With that, we remove from the $P(\theta)$ distributions the degeneracy related to the number of accessible orientational states. More importantly, the probabilities in Figure 5*B* are useful for a quantitative description of the free energy

associated with tilting the cholesterol molecule away from the membrane normal in various DMPC/Chol mixtures.

Specifically, we now define a "potential of mean force" (PMF)

$$\mathrm{PMF}(\theta) = -k_B T \ln \frac{P(\theta)}{P_0(\theta)} \tag{10}$$

Shown in Figure 5*C*, this PMF provides a measure of the free energy change associated with cholesterol tilt under different conditions, that is, $\Delta\mathrm{PMF}(\theta_1 - \theta_2) = \mathrm{PMF}(\theta_1) - \mathrm{PMF}(\theta_2)$ can be interpreted as the change in free energy due to tilting the Chol molecule from an angle θ_1 to an angle θ_2. Note that this free energy will generally contain energetic contributions as well as entropic contributions that are not associated with orientational degeneracy. As expected, Figure 5*C* illustrates that, for a fully random distribution of sterols found at equilibrium, the transition between different states is associated with no free energy cost (PMF = 0 for all θ). However, for realistic DMPC/Chol mixtures, as cholesterol density increases, for all $\theta_1 > \theta_2$ we find that PMF($\Delta\theta$) also increases with growing $\Delta\theta = \theta_1 - \theta_2$, indicating a greater penalty associated with rotating the Chol molecule some $\Delta\theta$ angle away from the membrane normal in Chol-rich bilayers.

The PMF we have defined here is closely related to the empirical free energy function used by Kessel et al.[19] to describe the transfer of a single cholesterol molecule from the aqueous phase into a lipid bilayer at an angle θ. Calculating the desolvation free energy of Chol as a function of the tilt angle, the authors found that the corresponding difference in free energy $G(\theta)$ produced a well-pronounced minimum at an angle $\theta = 0$, allowing for expansion of $G(\theta)$ around this point up to quadratic order in θ

$$G(\theta) = G^0 + \frac{1}{2}\chi\theta^2 \tag{11}$$

Here χ represents the tilt modulus of cholesterol, a quantitative measure of the force associated with tilting a molecule, and $G^0 = G(0)$. Kessel et al. noted that the validity of this expansion is generally restricted to the limit of large tilt modulus $\chi \gg k_B T$, where fluctuations in cholesterol orientation are small. Nevertheless, eq 11 provides a useful framework to discuss the influence of the different energetic contributions to cholesterol tilt.

Examining the PMF plots in light of the functional relationship given in eq 11 reveals that for lower tilt angles the PMFs indeed show a monotonic increase, which can be well approximated by a quadratic functional form. However, these plots clearly deviate from quadratic behavior for higher tilt angles, as they should, because expansion up to terms of θ^2 order as in eq 11 is valid only for small fluctuations in tilt angle around $\theta = 0$. Thus, a quadratic fit to the PMF plots for low tilt angles should provide a direct measure of the cholesterol tilt modulus, χ, that is responsible for aligning cholesterol in DMPC bilayers. The values of χ from the best fits to the PMF are presented as a function of Chol mole fraction in Figure 8. For each composition, fits were made in the angular range [8°, 20°] (see Computational Methods and Procedures) where sampling of cholesterol conformations was best, while still limiting the fit to the low angle regime. Error bars in Figure 8 were calculated from standard deviations obtained from similar fits to [8°, 12°], [12°, 16°], and [16°, 20°] intervals.

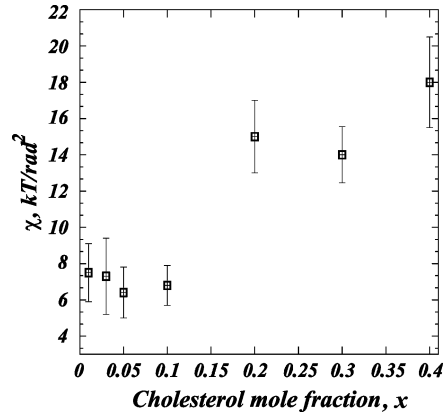

Figure 8. Tilt modulus of cholesterol, χ in DMPC bilayers as a function of sterol composition. For each model membrane, χ was obtained by fitting quadratic function to the PMF plots in Figure 5*C* in the angular range of $\theta \in$ [8°; 20°]. The error bars represent standard deviations from the similar fits obtained over [8°; 12°], [12°; 16°], and [16°; 20°].

Figure 8 reveals a strong concentration-dependence of χ. While the cholesterol tilt modulus appears to be constant within numerical error for the 1−10% Chol concentration range, χ exhibits a rapid increase between 10 and 20% Chol, and then remains relatively unchanged upon further cholesterol addition. Larger χ values signify a higher energetic penalty for cholesterol molecules to be inserted in a tilted orientation into a lipid membrane. It is likely that the high and relatively constant tilt modulus in the 20−40% mixtures is related to the fact that the DMPC/cholesterol membrane thickness reaches saturation levels at 20% Chol (Figure 3). Thus, significant energy must be spent to add an additional cholesterol with a tilted orientation into these mixtures. For low Chol concentrations, on the other hand, DMPC/Chol bilayers are relatively disordered. Therefore, insertion of a tilted cholesterol molecule can be less costly energetically, as cholesterol molecules are largely noninteracting. As a result, the cholesterol tilt modulus is relatively low. Interestingly, χ varies significantly (by ~6 $k_B T$/rad^2) between 10 and 20% Chol mixtures. Such a sudden increase in the tilt modulus can be attributed to the appearance of the Chol-rich liquid-order state when the system transitions from 10 to 20% Chol. Taken together, our results suggest that a change in cholesterol tilt modulus upon increasing Chol concentration is closely related to the state of fluidity of lipid−cholesterol membranes.

Relation to Function of Transmembrane Domains, the Examples of G-Protein-Coupled Receptors (GPCRs) and Antimicrobial Peptides. Cholesterol tilt may affect not only the organization of the lipid matrix, but can also regulate the function and stability of transmembrane (TM) domains, such as GPCRs or TM peptides. Recent microsecond-scale MD simulation of the prototypical GPCR, rhodopsin, in cholesterol-containing membrane environment[73] found cholesterols around the GPCR in a tilted conformation. Furthermore, dynamics in Chol tilt were linked to critical activation elements in GPCR,[73] such as local helical distortions and kinks, ultimately leading to more global transmembrane helix movements. A recent experimental study of the nanoscale organization of the β_2-adrenergic GPCR and its signaling partners,[74] on the other hand, revealed that, in the basal state, GPCRs were homogeneously distributed between ordered lipid rafts and disordered nonraft membrane compartments, whereas partner G-proteins were found predominantly in ordered rafts. Upon Chol depletion, rafts were disrupted, leading to the release of a sequestered pool of

G-proteins,[74] which then became available to interact with the partner GPCR to trigger a signaling cascade.

From this study, it appears that GPCR activation proceeds in membrane regions low in cholesterol content, where our study finds a higher probability for Chol tilt. It is reasonable to suspect, therefore, that the tilting of cholesterol around GPCR may be a crucial component in proper receptor functioning.

Cholesterol has been thought to have a mechanistic effect on the dynamics of antimicrobial TM peptides as well, such as pardaxin. NMR studies of membrane disruption by pardaxin[75] suggested that increased Chol concentration reduces the peptide's orientational freedom in the membrane and alters its preferred orientation. The authors hypothesized that pardaxin in Chol-rich systems is oriented along the membrane normal, and thus, its channel-forming activity is suppressed in high cholesterol concentrational mixtures. Our findings suggest that the orientational freedom of TM peptides in Chol-enriched membrane domains could be strongly influenced by the aligning field induced by cholesterols, which would enforce an orientational preference for pardaxin along the membrane normal. Alternatively, a higher concentration of cholesterol could altogether prevent the membrane insertion of the peptide.[75] Work toward establishing the role of cholesterol in membrane targeting by antimicrobial peptides is ongoing.

Concluding Remarks

To investigate the effect of cholesterol concentration on sterol orientation in phospholipid membranes, we have performed MD simulations on hydrated DMPC/cholesterol bilayers of various Chol compositions. In so doing, our aim was to relate cholesterol tilt to overall organization in phospholipid-Chol bilayers. We analyzed the cholesterol orientation at various cholesterol contents using, to our knowledge, the first estimates of cholesterol tilt modulus χ in lipid membranes from MD simulations. Beyond providing valuable insights about the energetics of cholesterol orientation in phospholipid bilayers, this empirical parameter should become a useful quantitative measure when developing more coarse-grained force fields to describe cholesterol interaction with lipid bilayers. On a practical note, we believe that the procedure used here to obtain χ from MD simulations can be routinely applied to estimate the tilt modulus of any rigid molecule inserted into lipid membranes.

We have verified the quality of the presented MD simulations by obtaining a remarkable fit between experimental and model form factors for all studied mixtures (Figure 2) as well as between other important structural data derived from simulations and experiments (Figures 3 and 4).

A detailed analysis of cholesterol tilt angle distributions in DMPC membranes revealed many instances when Chol molecules transiently oriented perpendicular to the bilayer normal. We showed that as Chol concentration increases, a change in average cholesterol orientation strongly (anti)correlates with the concomitant increase in membrane thickness. Thus, we concluded that the sterol tilt may be an important factor capable of inducing membrane ordering. These results are in agreement with MD studies by Aittoniemi et al.[22] who found similar correlations between the instantaneous tilt angle of a sterol and the average molecular order parameter of neighboring lipid chains in 20% DPPC−Chol and DOPC−Chol mixtures. Our simulations show that the correlation between cholesterol tilt and membrane ordering persisted over the entire 1−40% cholesterol concentration range that we have studied.

With that we proposed a possible mechanism of cholesterol alignment upon increasing concentration that may be responsible for the overall order in DMPC−Chol membranes. We have, therefore, established a link between cholesterol orientation and the well-known lipid condensing effect. Specifically, at low sterol concentrations (1−5% Chol), cholesterol is tilted mainly because of the entropic tendency to assume the maximum number of accessible states. As the sterol content increases, the cholesterol probability density distributions become narrower and appear to develop a well-defined maximum at lower tilt angles, indicating alignment of cholesterol molecules along the bilayer normal. This behavior is analogous to the isotropic−nematic transition observed in liquid crystals and can be the result of the interplay between entropic contributions, which tends to orient cholesterol molecules randomly, as well as unfavorable cholesterol−cholesterol pairwise interactions.

We note that the observed rapid change in χ between 10−20% can be explained by the appearance of the liquid-ordered state. In this Chol-rich fluidity state, phospholipid−cholesterol bilayers become ordered, Chol molecules align, and the membrane increases in thickness. Thus, in crowded cholesterol environments such as the liquid-ordered state, there is substantial loss in the orientational entropy of Chol molecules that is sacrificed to maintain a larger degree of translational entropy, as well as more favorable chol−lipid energetic interactions. Therefore, adding additional tilted Chol molecules into these bilayers will be accompanied by a high free-energy penalty. As a result, the tilt modulus increases.

To conclude, our analysis suggests that a change in cholesterol tilt modulus upon increasing Chol concentration is closely related to the state of fluidity of lipid−cholesterol membranes. It will be interesting to link these findings to changes in membrane material properties and to the way that lipids affect the proteins that are embedded within them, and work along these lines is ongoing.

Acknowledgment. G.K. is supported by grants from the National Institutes of Health P01 DA012408 and P01 DA012923. D.H. acknowledges the support from the Israel Science Foundation (ISF, Grant Nos. 1011/07 and 1012/07). The Fritz Haber research center is supported by the Minerva Foundation, Munich, Germany. Computational resources of the David A. Cofrin Center for Biomedical Information in the HRH Prince Alwaleed Bin Talal Bin Abdulaziz Alsaud Institute for Computational Biomedicine are gratefully acknowledged.

References and Notes

(1) Yeagle, P. L. *The biophysics and cell biology of cholesterol: an hypothesis for the essential role of cholesterol in mammalian cells. In Cholesterol in Membrane Models*; CRC Press: Boca Raton, FL., 1993; pp 1−12.

(2) Liscum, L.; Underwood, K. W. *J. Biol. Chem.* **1995**, *270*, 15443.

(3) Liscum L, L.; Munn, N. J. *Biochim. Biophys. Acta.* **1999**, *1438*, 19.

(4) Simons K, K.; Ikonen, E. *Science* **2000**, *290*, 1721.

(5) Mouritsen, O. G.; Zuckermann, M. J. *Lipids* **2004**, *39*, 1101.

(6) Rukmini, R.; Rawat, S. S.; Biswas, S. C.; Chattopadhyay, A. *Biophys. J.* **2001**, *81*, 2122.

(7) Schroeder, F. F.; Woodford, J. K.; Kavecansky, J.; Wood, W. G.; Joiner, C. *Mol. Membr. Biol.* **1995**, *21*, 113.

(8) Schroeder, F. F.; Frolov, A. A.; Murphy, E. J.; Atshaves, B. P.; Jefferson, J. R.; Pu, L.; Wood, W. G.; Foxworth, W. B.; Kier, A. B. *Proc. Soc. Exp. Biol. Med.* **1996**, *213*, 150.

(9) Simons, K.; Ikonen, E. *Nature* **1997**, *387*, 569.

(10) Xu, X.; London, E. *Biochemistry* **2000**, *39*, 843.

(11) Schroeder, F.; Nemecz, G.; Wood, W. G.; Joiner, C.; Morrot, G.; Ayraut-Jarrier, M.; Devaux, P. F. *Biochim. Biophys. Acta* **1991**, *1066*, 181.

(12) Epand, R. M. *Prog. Lipid Res.* **2006**, *45*, 279.

(13) Bloom, M.; Evans, E.; Mouritsen, O. G. *Q. Rev. Biophys.* **1991**, *24*, 293.

(14) Weihs, D.; Schmidt, J.; Goldiner, I.; Danino, D.; Rubin, M.; Talmon, Y.; Konikoff, F. M. *J. Lipid Res.* **2005**, *46*, 942.

(15) Troup, G. M.; Xie, Y.; Boesze-Battaglia, K.; Huang, Y.; Kirk, T.; Hanley, F.; Tulenko, T. N. *Macromol. Symp.* **2004**, *219*, 25.
(16) Harroun, T. A.; Katsaras, J.; Wassall, S. R. *Biochemistry* **2006**, *45*, 1227.
(17) Léonard, A.; Esrive, C.; Laguerre, M.; Pebay-Peyroula, E.; Néri, W.; Pott, T.; Katsaras, J.; Dufour, E. J. *Langmuir* **2001**, *17*, 2019.
(18) Marsan, M. P.; Muller, I.; Ramos, C.; Rodriguez, F.; Dufourc, E. J.; Czaplicki, J.; Milon, A. *Biophys. J.* **1999**, *76*, 351.
(19) Kessel, A.; Ben-Tal, N.; May, S. *Biophys. J.* **2001**, *81*, 643.
(20) Pasenkiewicz-Gierula, M.; Róg, T.; Kitamura, K.; Kusumi, A. *Biophys. J.* **2000**, *78*, 1376.
(21) Róg, T.; Pasenkiewicz-Gierula, M.; Vattulainen, I.; Karttunen, M. *Biochim. Biophys. Acta* **2008**, doi: 10.1016/j.bbamem.2008.08.022.
(22) Aittoniemi, J.; Róg, T.; Pasenkiewicz-Gierula, M.; Karttunen, M.; Vattulainen, I. *J. Phys. Chem B.* **2006**, *110*, 25562.
(23) Smondyrev, A. M.; Berkowitz, M. L. *Biophys. J.* **2001**, *80*, 1649.
(24) Czub, J.; Baginski, M. *Biophys. J.* **2006**, *90*, 2368.
(25) Pandit, S. A.; Bostick, D.; Berkowitz, M. L. *Biophys. J.* **2004**, *86*, 1345.
(26) Kučerka, N.; Perlmutter, J. D.; Pan, J.; Tristram-Nagle, S.; Katsaras, J.; Sachs, J. N. *Biophys. J.* **2008**, *95*, 2792.
(27) Almeida, P. F. F.; Vaz, W. L. C.; Thompson, T. E. *Biochemistry* **1992**, *31*, 6739.
(28) Greenwood, A. I.; Tristam-Nagle, S.; Nagle, J. F. *Chem. Phys. Lipids* **2006)** , *143*, 1.
(29) Hung, W. C.; Lee, M. T.; Chen, F. Y.; Huang, H. W. *Biophys. J.* **2007**, *92*, 3960.
(30) de Gennes, P. G.; Prost, J. *The physics of liquid crystals*; Clarendon Press: Oxford, 1993.
(31) Kramer, D.; Ben-Shaul, A.; Chen, Z.-Y.; Gelbart, W. M. *J. Chem. Phys.* **1992**, *96*, 2236.
(32) Hodzic, A.; Rappolt, M.; Amenitsch, H.; Laggner, P.; Pabst, G. *Biophys. J.* **2008**, *94*, 3935.
(33) Pan, J.; Mills, T. T.; Tristam-Nagle, S.; Nagle, J. F. *Phys. Rev. Lett.* **2008**, *100*, 198103.
(34) Tulenko, T. N.; Chen, M.; Mason, P. E.; Mason, R. P. *J. Lipid Res.* **1998**, *39*, 947.
(35) Chiu, S.-W.; Pandit, S. A.; Scott, H. L.; Jakobsson, E. *J. Phys. Chem. B* **2009**, *113*, 2748.
(36) Berendsen, H.; van der Spoel, D.; vad Drunen, R. *Comput. Phys. Commun.* **1995**, *91*, 43.
(37) Lindahl, E.; Hess, B.; van der Spoel, D. *J. Mol. Model.* **2001**, *7*, 306.
(38) Hess, B.; Bekker, H.; Berendsen, H. J. C.; Fraaige, J. G. E. M. *J. Comput. Chem.* **1997**, *18*, 1463.
(39) Essmann, U.; Perera, L.; Berkowitz, M. L.; Darden, T.; Lee, H.; Pedersen, L. G. *J. Chem. Phys.* **1995**, *103*, 8577.
(40) Nose, S.; Klein, M. L. *Mol. Phys.* **1983**, *50*, 1055.
(41) Parrinello, M.; Rahman, A. *J. Appl. Phys.* **1981**, *52*, 182.
(42) Evans, D. J.; Holian, B. L. *J. Chem. Phys.* **1985**, *83*, 4069.
(43) Pandit, S. A.; Chiu, S.-W.; Jakobsson, E.; Grama, A.; Scott, H. L. *Langmuir* **2008**, *24*, 6858.
(44) Pabst, G. *Biophys. Rev. Lett.* **2006**, *1*, 57.
(45) Pabst, G.; Rappolt, M.; Amenitsch, H.; Laggner, P. *Phys. Rev. E* **2000**, *62*, 4000.
(46) Pabst, G.; Koschuch, B.; Pozo-Navas, B.; Rappolt, M.; Lohner, K.; Laggner, P. *J. Appl. Crystallogr.* **2003**, *63*, 1378.
(47) Zhang, R.; Suter, R. M.; Nagle, J. F. *Phys. Rev. E* **1994**, *50*, 5047.
(48) Rappolt, M.; Vidal, M. F.; Kriechbaum, M.; Steinhart, M.; Amentisch, H.; Bernstorff, S.; Laggner, P. *Eur. Biophys. J.* **2003**, *31*, 575.
(49) Gallova, J.; Uhrikova, D.; Hanulova, J.; Teixeria, J.; Balgavy, P. *Colloids Surf., B* **2004**, *38*, 11.
(50) McIntosh, T. J. *Biochim. Biophys. Acta* **1978**, *513*, 43.
(51) de Meyer, F.; Smit, B. *Proc. Natl. Acad. Sci. U.S.A.* **2009**, *106* (10), 3654.
(52) Douliez, J.-P.; Léonard, A.; Dufourc, E. J. *Biophys. J.* **1995**, *68*, 1727.
(53) Douliez, J.-P.; Léonard, A.; Dufourc, E. J. *J. Phys. Chem.* **1996**, *100*, 18450.
(54) Urbina, J. A.; Peterar, S.; Le, H.-b.; Patterson, J.; Montez, B.; Oldfield, E. *Biochim. Biophys. Acta* **1995**, *1238*, 163.
(55) Urbina, J. A.; Moreno, B.; Arnold, W.; Taron, C. H.; Orlean, P.; Oldfield, E. *Biophys. J.* **1998**, *75*, 1372.
(56) Nielsen, M.; Thewalt, J.; Miao, L.; Ipsen, J. H.; Bloom, M.; Zuckermann, M. J.; Mouritsen, O. G. *Europhys. Lett.* **2000**, *52*, 368.
(57) Sankaram, M. B.; Thompson, T. E. *Biochemistry* **1990**, *29*, 10676.
(58) Róg, T.; Pasenkiewicz-Gierula, M. *Biophys. Chem.* **2004**, *107*, 151.
(59) Jedlovsky, P.; Mezei, M. *J. Phys. Chem. B.* **2003**, *107*, 5311.
(60) Róg, T.; Pasenkiewicz-Gierula, M. *Biophys. J.* **2001**, *81*, 2190.
(61) Pasenkiewicz-Gierula, M.; Subczynski, W. K.; Kusumi, A. *Biochemistry* **1990**, *29*, 4059.
(62) Murari, R.; Murari, M. P.; Baumann, W. J. *Biochemistry* **1986**, *25*, 1062.
(63) Khelashvili, G.; Pandit, S. A.; Scott, H. L. *J. Chem. Phys.* **2005**, *123*, 034910.
(64) Subramaniam, S.; McConnell, H. M. *J. Phys. Chem.* **1987**, *91*, 1715.
(65) Gershfeld, N. L. *Biophys. J.* **1978**, *22*, 469.
(66) Vroege, G. J.; Lekkerkerker, H. N. W. *Rep. Prog. Phys.* **1992**, *55*, 1241.
(67) Almeida, P. F. F.; Wiegel, F. W. *J. Theor. Biol.* **2006**, *238*, 269.
(68) Zhang, Z.; Lu, L.; Berkowitz, M. L. *J. Phys. Chem. B* **2008**, *112*, 3807.
(69) Bennett, W. F. D.; MacCallum, J. L.; Hinner, M. J.; Marrink, S. J.; Tieleman, D. P. *J. Am. Chem. Soc.* **2009**, *131*, 12714.
(70) Kučerka, N.; Marquardt, D.; Harroun, T. A.; Nieh, M. P.; Wassall, S. R.; Katsaras, J. *J. Am. Chem. Soc.* **2009**, *131*, 16358.
(71) Olsen, B. N.; Schlesinger, P. H.; Baker, N. A. *J. Am. Chem. Soc.* **2009**, *131*, 4854.
(72) Ivankin, A.; Kuzmenko, I.; Gidalevitz, D. *Phys. Rev. Lett.* **2010**, *104*, 108101.
(73) Khelashvili, G.; Grossfield, A.; Feller, S. E.; Pitman, M. C.; Weinstein, H. *Proteins: Struct., Funct., Bioinf.* **2009**, *76*, 403.
(74) Pontier, S. M.; Percherancier, Y.; Galandrin, S.; Breit, A.; Gales, C.; Bouvier, M. *J. Biol. Chem.* **2008**, *283*, 24659.
(75) Ramomoorthy, A.; Lee, D.-K.; Narasimhaswamy, T.; Nanga, R. P. R. *Biochim. Biophys. Acta* **2009**, doi: 10.1016/j.bbamem.2009.08.012.

JP101889K